PERGAMON

International Journal of Heat and Mass Transfer 45 (2002) 2303–2314

International Journal of HEAT and MASS TRANSFER

www.elsevier.com/locate/ijhmt

Analysis of heat transfer in the rapid thermal processing of the plasma display panel

Man Yeong Ha [a,*], Kong Hoon Lee [b], Moon Gun Bae [a], Jong Rae Cho [c], Hee Seung Lee [d], Jin Ho Choi [d]

[a] *School of Mechanical Engineering, Pusan National University, San 30, Jangjeon-Dong, Kumjung-Ku, Pusan 609-735, South Korea*
[b] *Korea Institute of Machinery and Materials, 171 Jang-Dong, Yusung-Ku, Taejon 305-343, South Korea*
[c] *School of Mechanical and Information Engineering, Korea Maritime University, #1, dongsam Dong, Yeongdo-Gu, Pusan 606-791, South Korea*
[d] *LG Production Engineering Research Center, 19-1, Cheongho-Ri, Jinwuy-Myun, Pyungtaek-Si, Kyunggi-Do, 451-713, South Korea*

Received 23 May 2001; received in revised form 12 October 2001

Abstract

Numerical analysis has been carried out to analyze the combined conductive and radiative heat transfer in the annealing process using the RTP system. The finite volume and discrete ordinates methods are used to solve the energy and radiative transfer equations, respectively. The temperature distribution in the panel depends strongly on the operating conditions. The process depends on the operating conditions such as lamp intensity, panel transport velocity, process length, ambient gas temperatures, etc. The temperature in the RTP section increases very rapidly first due to the intensive radiant heating and reaches the maximum. However the temperature decreases after the opaque dielectric is changed to a semi-transparent medium. The temperature differences/gradients of the panel are small in the pre-heating and post-heating sections but are very large in the RTP section, which may result in the large thermal stress and displacement to cause the considerable damage of the panel. Thus, the simulations using the present computer program are useful to obtain the optimal operating conditions and to produce the panel of good quality.

1. Introduction

Plasma display panel (PDP) is a display device using the the plasma generated by the electric discharge of gas and consists of the glass coated with the dielectric and many electrodes. During the PDP manufacturing process, there is an annealing process to heat the panel using the high temperature heat sources. To control the annealing process properly is very important to produce the panel of high quality. The furnace has usually been used to provide the enough heat during the annealing process. However, the annealing by furnace has some problems to require large spaces and takes long process time, increasing the cost and decreasing the productivity [1,2].

Recently, rapid thermal processing (RTP) is suggested as an alternative way to replace the conventional annealing process using furnace. Compared to the conventional furnace annealing process, RTP takes shorter process time, requires smaller areas and is more stable to the external disturbance. Thus, RTP is expected to make rapid progress in the PDP productivity and is expected to become the next generation annealing process for the PDP. However, we should solve some problems caused by the process system such as the temperature non-uniformity in the panel due to the rapid heating, and thermal stress and displacement due to this the non-uniformity of temperature [3,4].

In order to develop the optimal RTP system for the PDP annealing process, we should understand the

* Corresponding author. Tel.: +82-51-510-2440; fax: +82-51-512-9835.
E-mail address: myha@hyowon.pusan.ac.kr (M.Y. Ha).

0017-9310/02/$ - see front matter
PII: S0017-9310(01)00326-X

Nomenclature

c	specific heat (kJ/kg K)
F	view factor
G_λ	spectral irradiance (W/m^2 μm)
h	heat transfer coefficient (W/m^2 K)
H	thickness of the medium (m)
I_λ	spectral radiative intensity (W/m^2 μm)
$I_{b\lambda}$	blackbody intensity (W/m^2 μm)
k	thermal conductivity (W/m K)
n	refractive index
q	heat flux (W/m^2)
q^r	radiative heat flux (W/m^2)
$\mathbf{q}^r$	radiative flux vector (W/m^2)
$\mathbf{r}$	position vector (m)
T	temperature (K)
x, y, z	coordinates (m)

Greek letters

ε	emissivity
η, ξ	dummy coordinates
κ	absorption coefficient (m^{-1})
λ	wavelength (μm)
λ_c	cut-off wavelength (μm)
ρ	density (kg/m^3), reflectivity
θ, ϕ	polar and azimuthal angles
Ω	solid angle (sr)
$\mathbf{\Omega}$	directional vector

Superscripts

0	refers to the incident flux from the xenon lamp
1	refers to the incident flux from the halogen lamp
+	refers to the hemispherical value in the positive direction
−	refers to the hemispherical value in the negative direction
′	refers to the incident value

Subscripts

0	refers to the bottom surface ($y = 0$)
1	refers to the glass substrate
2	refers to the dielectric
amb	refers to the ambient
c	refers to the critical angle defined by Snell's law
in	refers to the incident radiation
sur	refers to the surroundings
x	refers to the value in the x-direction
y	refers to the value in the y-direction
λ	refers to the spectral quantity

detail physics associated with the RTP system. The most important heat transfer mode in the RTP system is the radiative heat transfer. The radiative heat transfer is a very complex phenomenon and depends on the wavelength, direction and temperature. In order to obtain the temperature distribution in the panel, we should analyze the combined conductive and radiative heat transfer in the panel. The radiative properties of heat sources and panel are expressed as a function of wavelength and temperature. In the present study, we developed a computer program to analyze the combined conductive and radiative heat transfer in the annealing process using the RTP system. The temperature distribution in the panel is obtained as a function of time for different operating conditions. The temperature distribution is also used to determine the thermal stress and displacement of the panel to determine the optimal operating conditions using the RTP system.

2. Mathematical model

2.1. Model equations of conductive–radiative heat transfer

Fig. 1 shows the schematic of a RTP annealing system used in the present study. The annealing process is divided into three parts of pre-heating, RTP and post-heating sections. Halogen lamps in the pre-heating and posting sections and xenon lamps in the RTP section are used to heat the panel. The panel moves at a constant speed in the horizontal direction from the pre- to post-heating section in between the lamps located at in the upper and lower parts of the RTP annealing system. The dielectric coated on the glass substrate is initially opaque to radiation but the dielectric becomes semi-transparent to radiation by the intensive radiant heating in the RTP section. It is assumed that the dielectric is changed to a semi-transparent medium when the temperature of dielectric reaches 650 °C.

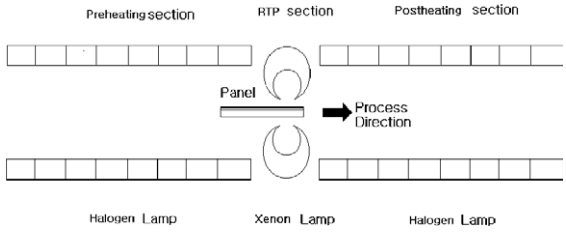

Fig. 1. Schematic of the RTP annealing process.

When the dielectric is opaque to radiation, it absorbs and reflects the radiation energy only on the surface but the glass substrate absorbs the radiation energy inside the medium since the glass is semi-transparent to radi-

ation. When both the dielectric and glass substrate are semi-transparent to radiation, the large fraction of the incident radiation energy is transmitted through the panel, which will results in the decrease of temperature in the post-heating section.

In addition, the following assumptions are made in the analysis: (1) ambient gas is assumed to be transparent to radiation and has the refractive index of unity; (2) the semi-transparent media emit and absorb but does not scatter thermal radiation; (3) the media are in thermodynamic equilibrium for which Planck's and Kirchhoff's laws are valid; (4) the spatial dimensions of the media are much longer than the wavelength of radiation for the semi-transparent band even though the thickness of the dielectric is very small, i.e., the coherence effects are negligible; (5) the interface between the semi-transparent medium and the bounding entity is optically smooth; (6) the opaque dielectric and lamps are gray diffuse emitters of radiation.

The two-dimensional computational domain in the horizontal (x) and thickness (y) direction is used in the present study, as shown in Fig. 2. Because the length of lamps in the width (z) direction is long enough to cover the panel, the temperature variation in the z-direction is neglected.

The two-dimensional energy equation to govern the temperature distribution in the panel is defined as

$$\rho c\frac{\partial T}{\partial t}=\frac{\partial}{\partial x}\left(k\frac{\partial T}{\partial x}\right)+\frac{\partial}{\partial y}\left(k\frac{\partial T}{\partial y}\right)+\nabla\cdot\mathbf{q}^{\mathrm{r}}, \tag{1}$$

where ρ, c, k and T represent the density, specific heat, thermal conductivity and temperature of the panel, respectively. The divergence of the radiative heat flux vector is defined by

$$\begin{aligned}\nabla\cdot\mathbf{q}^{\mathrm{r}}&=\int_0^\infty \nabla\cdot\mathbf{q}_\lambda^{\mathrm{r}}\,\mathrm{d}\lambda\\&=\int_0^\infty \kappa_\lambda[4\pi n_\lambda^2 I_{b\lambda}(T)-G_\lambda]\,\mathrm{d}\lambda.\end{aligned} \tag{2}$$

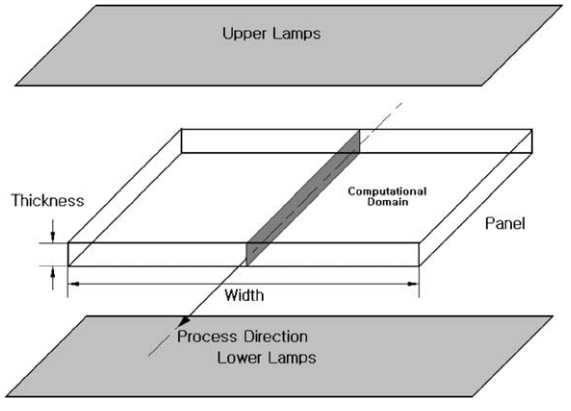

Fig. 2. Two-dimensional computational domain.

The spectral radiative flux vector $\mathbf{q}_\lambda^{\mathrm{r}}$ and the spectral irradiance G_λ are defined as

$$\mathbf{q}_\lambda^{\mathrm{r}}=\int_{\Omega=4\pi} I_\lambda(\mathbf{r},\mathbf{\Omega})\mathbf{\Omega}\,\mathrm{d}\Omega \tag{3}$$

and

$$G_\lambda=\int_{\Omega=4\pi} I_\lambda(\mathbf{r},\mathbf{\Omega})\,\mathrm{d}\Omega, \tag{4}$$

respectively. $I_\lambda(\mathbf{r},\mathbf{\Omega})$ denotes the spectral radiative intensity that depends on the wavelength λ, spatial position vector $\mathbf{r}$, and direction cosine vector $\mathbf{\Omega}$. $I_{b\lambda}(T)$ is the blackbody radiative intensity that depends only on temperature. The divergence of the radiative flux vector defined in Eq. (2) is obtained by solving the radiative transfer equation (RTE) within the semi-transparent medium [5].

The opaque dielectric coated on the glass substrate enters the pre-heating section and then is changed to a semi-transparent medium by being heated in the RTP section. If the dielectric is semi-transparent to radiation, the divergence of the radiative flux vector $\nabla\cdot\mathbf{q}^{\mathrm{r}}$ should be considered within the dielectric as well as in the glass substrate. However, if the dielectric is opaque, radiation incident on the surface of the dielectric cannot be transmitted through the dielectric and the reflection and absorption processes occur only at the surface of dielectric. Then the radiation exchange is considered as boundary conditions when the energy equation is solved.

Fig. 3 shows the schematic of the dielectric coated on the surface of the glass substrate. When the panel enters the pre-heating zone, the dielectric is opaque. Thus, the boundary conditions in the y-direction for the opaque dielectric are defined as follows:

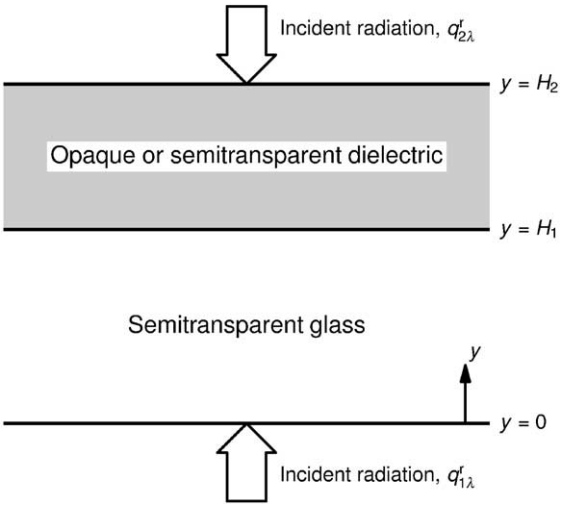

Fig. 3. Schematic of dielectric coated on the glass.

$$k_1 \left.\frac{dT}{dy}\right|_{y=0} = h_1(T_0 - T_{amb}) + \int_{\lambda_c}^{\infty} \varepsilon_{1\lambda}\pi I_{b\lambda}(T_0)\,d\lambda - \int_{\lambda_c}^{\infty} \varepsilon_{1\lambda} q^{r}_{1\lambda,in}\,d\lambda \quad \text{at } y = 0, \tag{5}$$

$$-k_2 \left.\frac{dT}{dy}\right|_{y=H_1} = -k_1 \left.\frac{dT}{dy}\right|_{y=H_1} - \int_{0}^{\lambda_c} \varepsilon_{2\lambda}\pi I_{b\lambda}(T_{H_1})\,d\lambda + \int_{0}^{\lambda_c} \varepsilon_{2\lambda} q^{r+}_{1\lambda}\big|_{H_1}\,d\lambda \quad \text{at } y = H_1, \tag{6}$$

$$-k_2 \left.\frac{dT}{dy}\right|_{y=H_2} = h_2(T_{H_2} - T_{amb}) + \int_{0}^{\infty} \varepsilon_{2\lambda}\pi I_{b\lambda}(T_{H_2})\,d\lambda - \int_{0}^{\infty} \varepsilon_{2\lambda} q^{r}_{2\lambda,in}\,d\lambda \quad \text{at } y = H_2, \tag{7}$$

where h, T_{amb}, λ_c and ε represent the heat transfer coefficient, ambient gas temperature, cut-off wavelength and emissivity, respectively. The cut-off wavelength λ_c indicates the wavelength for which the medium is considered to be opaque to radiation. λ_c is 5 μm and assumed to be the same for the glass and dielectric. The emissivity $\varepsilon_{1\lambda}$ is 0.9 for the spectral range where the glass is considered to be opaque. The emissivity $\varepsilon_{2\lambda}$ is 0.996 for both $0 \leqslant \lambda \leqslant \lambda_c$ and $\lambda_c \geqslant \infty$. The emissivities are also listed in Table 1.

If the temperature of the dielectric reaches 650 °C in the RTP section, it is assumed that the opaque dielectric is changed to a semi-transparent medium. Thus, if the dielectric is semi-transparent, the boundary conditions given in Eqs. (6) and (7) should be changed, respectively, as follows:

$$-k_2 \left.\frac{dT}{dy}\right|_{H_1} = -k_1 \left.\frac{dT}{dy}\right|_{H_1} \quad \text{at } y = H_1, \tag{8}$$

$$-k_2 \left.\frac{dT}{dy}\right|_{y=H_2} = h_2(T_{H_2} - T_{amb}) + \int_{\lambda_c}^{\infty} \varepsilon_{2\lambda}\pi I_{b\lambda}(T_{H_2})\,d\lambda - \int_{\lambda_c}^{\infty} \varepsilon_{2\lambda} q^{r}_{2\lambda,in}\,d\lambda \quad \text{at } y = H_2. \tag{9}$$

The symmetry boundary conditions are used at $x = 0$ and L. The room temperature is used as an initial condition of the panel.

Table 1
The thermophysical properties of the glass substrate and the dielectric substance

	Glass	Dielectric
Thickness (mm)	2.8	0.025
Density (kg/m^3)	2514.8	2500
Thermal conductivity (W/m K)	1.3272	0.677
Specific heat (J/kg K)	1120.9	556.3
Emissivity (ε)	0.9	0.996

2.2. Radiative transfer model

The RTE for a spectrally absorbing–emitting medium can be written as [6]

$$(\mathbf{\Omega}\cdot\nabla) I_\lambda(\mathbf{r},\mathbf{\Omega}) = \kappa_\lambda[n_\lambda^2 I_{b\lambda}(T) - I_\lambda(\mathbf{r},\mathbf{\Omega})] \tag{10}$$

The boundary conditions for Eq. (10) are defined as follows for the optically smooth surface:

$$I_\lambda(\mathbf{r},\mathbf{\Omega}) = [1-\rho_\lambda(\theta)]\frac{n_\lambda^2}{n_{\lambda,in}^2} I_{\lambda,in} + \rho_\lambda(\theta) I_\lambda(\mathbf{r},\mathbf{\Omega}'), \tag{11}$$

where n is the refractive index. ρ_λ in Eq. (11) is the reflectivity at the interface between two media having different refractive indices and is obtained by combining Snell's law for refraction and Fresnel's equation for reflection [5]:

$$\rho_\lambda(\theta) = \begin{cases} 1.0 & \text{for } \theta \geqslant \theta_c, \\ \frac{1}{2}\left(\frac{n_{\lambda,in}\cos\theta - n_\lambda P}{n_{\lambda,in}\cos\theta + n_\lambda P}\right)^2 + \frac{1}{2}\left(\frac{n_\lambda\cos\theta - P}{n_\lambda\cos\theta + P}\right)^2 & \text{for } \theta < \theta_c, \end{cases} \tag{12}$$

where $P = \sqrt{n_{\lambda,in}^2 - n_\lambda^2(1-\sin^2\theta)}$ and $\theta = \cos^{-1}(\mathbf{\Omega}\cdot\mathbf{n})$. θ_c is the critical angle given by the Snell's law as $\theta_c = \sin^{-1}(n_{\lambda,in}/n_\lambda)$. If both the dielectric and glass are semi-transparent as shown in Fig. 4, $I_{\lambda,in}$ in Eq. (11) can be written as [7]

$$y = 0: \quad I_{\lambda,in} = I^0_{1\lambda}\delta(\cos\theta_0 - 1) + I^1_{1\lambda} + I_{b\lambda}(T_{sur}), \quad n_{\lambda,in} = 1, \quad \cos\theta_0 = \sqrt{1 - n_{1\lambda}^2\sin^2\theta_1}, \tag{13}$$

$$y = H_1^-: \quad I_{\lambda,in} = I_{2\lambda}(x, H_1, \theta_2, \phi), \quad n_{\lambda,in} = n_{2\lambda}, \quad \cos\theta_2 = -\sqrt{1 - (n_{1\lambda}/n_{2\lambda})^2\sin^2\theta_1}, \tag{14}$$

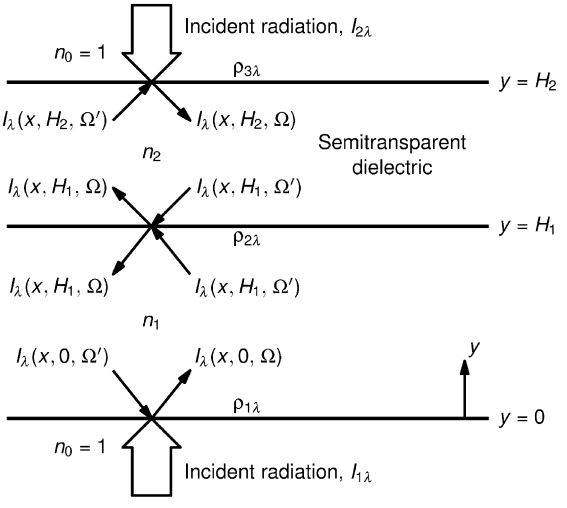

Fig. 4. Boundary conditions for the radiative transfer for the glass and semi-transparent dielectric.

$$y = H_1^+ : \; I_{\lambda,\mathrm{in}} = I_{1\lambda}(x, H_2, \theta_1, \phi),$$
$$n_{\lambda,\mathrm{in}} = n_{1\lambda}, \quad \cos\theta_1 = \sqrt{1 - (n_{2\lambda}/n_{1\lambda})^2 \sin\theta_2}, \tag{15}$$

$$y = H_2 : \; I_{\lambda,\mathrm{in}} = I^0_{2\lambda}\delta(\cos\theta_0 - 1) + I^1_{2\lambda} + I_{b\lambda}(T_{\mathrm{sur}}),$$
$$n_{\lambda,\mathrm{in}} = 1, \quad \cos\theta_0 = -\sqrt{1 - n^2_{2\lambda}\sin\theta_2}, \tag{16}$$

where $I^0_{1\lambda}\delta(\cos\theta_0 - 1)$ and $I^0_{2\lambda}\delta(\cos\theta_0 - 1)$ denote the collimated intensities incident on the bottom and top surfaces of the panel from the xenon lamps. The intensities from the xenon lamps are incident only on the part of surfaces in the RTP section as shown in Fig. 1. $I^1_{1\lambda}$ and $I^1_{2\lambda}$ denote the intensities incident on the bottom and top surfaces from the halogen lamps.

If the dielectric is opaque and glass is semi-transparent as shown in Fig. 5, radiative transfer related to the dielectric is confined on the surface and the RTE is solved only inside the glass substrate. Thus, Eq. (13) is used as the boundary condition at $y = 0$ and the interface condition at $y = H_1^-$ is as follows:

$$y = H_1^- : \; I_{\lambda,\mathrm{in}} = I_{b\lambda}(x, H_1), \quad n_{\lambda,\mathrm{in}} = 1,$$
$$\rho_\lambda = 1 - \varepsilon_{2\lambda}. \tag{17}$$

The radiative flux arrived at the infinitesimal element $\mathrm{d}A_i$ on the surface of panel from a lamp component A_j is defined with the assumption that the panel surfaces are relatively cold:

$$q^{\mathrm{r},0}_{\lambda,i} = \sum_{j=1}^{N_h} J_{\lambda,j} F_{\mathrm{d}A_i - A_j}. \tag{18}$$

The intensity incident on the surface can be defined as $I^0_{\lambda,i} = q^{\mathrm{r},0}_{\lambda,i}/\pi$. $J_{\lambda,j}$ is the spectral radiosity leaving the jth

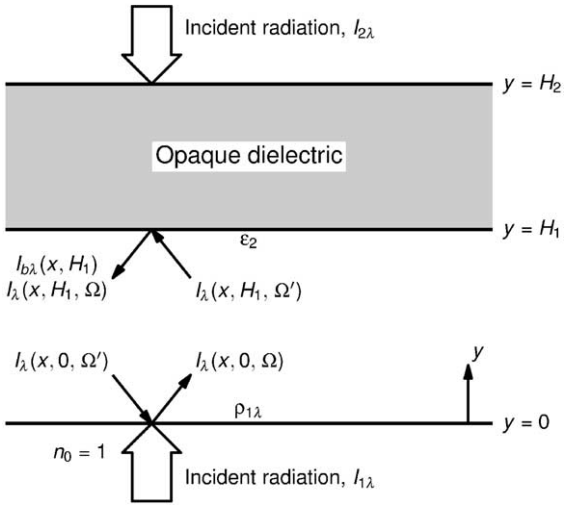

Fig. 5. Boundary conditions for the radiative transfer for the glass and opaque dielectric.

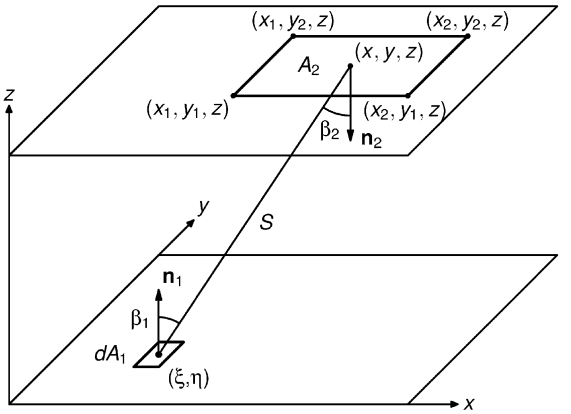

Fig. 6. Coordinate system and nomenclature to calculate the view factor.

lamp and the view factor $F_{\mathrm{d}A_i - A_j}$ for the geometry given in Fig. 6 is obtained by [8]

$$F_{\mathrm{d}A_i - A_j} = \frac{z^2}{\pi}\left[\left[\frac{(x-\xi)\tan^{-1}\left[(y-\eta)\Big/\sqrt{z^2 + (x-\xi)^2}\right]}{2z^2\sqrt{z^2 + (x-\xi)^2}} + \frac{(y-\eta)\tan^{-1}\left[(x-\xi)\Big/\sqrt{z^2 + (y-\eta)^2}\right]}{2z^2\sqrt{z^2 + (y-\eta)^2}}\right]_{x_1}^{x_2}\right]_{y_1}^{y_2}. \tag{19}$$

2.3. Thermophysical and radiative properties

The soda-lime glass is used as the substrate of the panel. The thermophysical properties of the soda-lime glass depend weakly on temperature [9] and the details of the properties of the dielectric are not known. Thus all the thermophysical properties are assumed to be independent of temperature and listed in Table 1. The density of the soda-lime glass is well-known and the thermal conductivity of the glass is evaluated using the experimental correlation given by Mann et al. [9]. The specific heat of the glass is approximated by combining the partial coefficients corresponding to the weight percents of chemical components of glass [10,11] and the same approximation is used to evaluate the thermal conductivity and specific heat of the dielectric. The weight percents of chemical components and the density of the dielectric is given by the manufacturer.

Radiative properties of the soda-lime glass reported by Rubin [12] are used which can also found elsewhere [13]. The temperature dependency of the absorption coefficient is not considered and the refractive index is fixed to 1.5. The radiative properties of the dielectric

coated on the glass are measured by the manufacturer of the PDP but are not shown here. The emissivities in the opaque spectral range are given in Table 1.

2.4. Method of solution

The finite volume method [14] is used to solve the energy equation (1) and the discrete ordinates method [6] to solve the radiative transfer equation (10). S_8 level symmetric quadrature is used for the discrete ordinates method. Details for the numerical technique is not explained here but can be found elsewhere [5,13,14].

Table 2 shows the operating conditions of the annealing process for the panel of 0.632 m size. Two different operating conditions "A" and "B" are examined to investigate the effects of lamp intensity on the temperature distribution in the panel. The lamp intensities for the process A are generally lower than those for the process B. Table 3 shows the operating conditions of the annealing process for the panel of 0.120 m size. The process lengths in the horizontal direction and transport velocities for the larger panel (0.632 m size) are greater than those for the smaller panel (0.120 m size) because the larger panel is heated more than the smaller panel. The lamp intensity fractions in Tables 2 and 3 represent the fractions used in the pre-heating, RTP and post-heating sections. Thus the lamp intensity fraction of 0.3 means that 30% of lamp capacity is used to heat the panel. The ambient temperatures in Tables 2 and 3 represent the gas temperatures in between the panel and lamps.

The number of grid points used in the present calculation is 101 in the x (horizontal) direction and 21 in the y (thickness) directions. The grid is non-uniform and is denser near the boundaries and interface between the dielectric and glass. The time-step Δt used for the numerical time integration is 1 s in the pre-heating and post-heating sections and 0.1 s in the RTP section.

Table 2
Operating conditions of the processes for the panel of 0.632 m size

	Pre-heating section				RTP section	Post-heating section			
	Zone 1	Zone 2	Zone 3	Zone 4		Zone 1	Zone 2	Zone 3	Zone 4
Process length (m)	1.0	1.0	1.5	1.5	0.1	1.5	1.5	1.5	1.5
Lamp intensity fraction									
Type A									
Upper	0.0	0.0	0.3	0.3	0.7	0.3	0.3	0.0	0.0
Lower	0.3	0.3	0.4	0.4	0.7	0.3	0.3	0.0	0.0
Type B									
Upper	0.0	0.0	0.7	0.9	1.0	0.3	0.3	0.2	0.2
Lower	0.3	0.5	0.7	0.9	1.0	0.3	0.3	0.2	0.2
Glass transport velocity (mm/s)	2.7				7.3	6.0			
Ambient gas temperature (°C)	400		500		600	500		400	

Table 3
Operating conditions of the processes for the panel of 0.12 m size

	Pre-heating section				RTP section	Post-heating section			
	Zone 1	Zone 2	Zone 3	Zone 4		Zone 1	Zone 2	Zone 3	Zone 4
Process Length (m)	0.264	0.264	0.396	0.396	0.1	0.396	0.396	0.264	0.264
Lamp intensity fraction									
Type A									
Upper	0.0	0.0	0.3	0.3	0.7	0.3	0.3	0.0	0.0
Lower	0.3	0.3	0.4	0.4	0.7	0.3	0.3	0.0	0.0
Type B									
Upper	0.0	0.0	0.7	0.9	1.0	0.3	0.3	0.2	0.2
Lower	0.3	0.5	0.7	0.9	1.0	0.3	0.3	0.2	0.2
Glass transport velocity (mm/s)	0.7				3.5	1.6			
Ambient gas temperature (°C)	400		500		600	500		400	

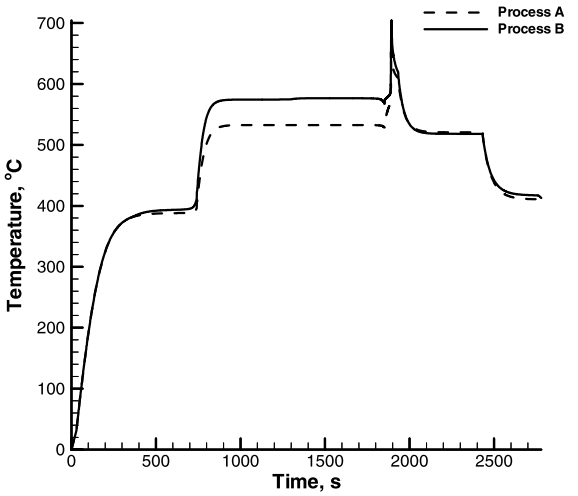

Fig. 7. Dielectric surface temperature variation as a function of time for different annealing processes of types A and B for the 0.632 m panel size.

3. Results and discussion

Fig. 7 shows the temperature variation at the center on the dielectric surface as a function of time for processes A and B in case of the panel of 0.632 m size as the panel moves from the pre-heating to the post-heating section. As shown in Table 2, the halogen lamp intensity fractions at the 1st and 2nd zones of the pre-heating section for the process A are 0.0 for the upper lamps and 0.3 for the lower ones. Thus, the dielectric surface temperature for the process A increases at the early part of the 1st and 2nd zones in the pre-heating section due to the radiant heating from the halogen lamps and convection heating from the ambient gas at the temperature of 400 °C. As the panel moves to the later part of the 1st and 2nd zones, temperature approaches the slightly lower value than the ambient gas temperature of 400 °C. The halogen lamp intensity fractions at the 3rd and 4th zones of the pre-heating section for the process A increases to 0.3 for the upper lamps and 0.4 for the lower ones. The ambient gas temperature at the 3rd and 4th zones of the pre-heating section is also increased to 500 °C. Thus, when the panel moves in the 3rd and 4th zones of the pre-heating section, the dielectric surface temperature increases rapidly again and then approaches slightly higher value than the ambient gas temperature of 500 °C. This uniform temperature period is very important in the annealing process and required to produce the panel of high quality. In the RTP section, the xenon lamp intensity fractions for the process A are 0.7 for both the lower and upper lamps. The ambient gas temperature and transport velocity in this section are increased to 600 °C and 7.3 mm/s, respectively. Since the intensity of xenon lamp is very intensive and the ambient gas temperature is high in the RTP section, the dielectric surface temperature increases very rapidly in comparison to that in the pre-heating section and then reaches the maximum. Thus, the thermal stress in this region is expected to be very large due to the large temperature gradient in the thickness direction. Since the opaque dielectric is changed to the semi-transparent medium when the temperature of dielectric is higher than 650 °C, the large fraction of radiation incident on the dielectric surface is transmitted through the panel, which results in the decrease of the surface temperature in the remaining RTP section. In the 1st and 2nd zones of the post-heating section for the process A, the halogen lamp intensity fractions decrease to 0.3 for both the upper and lower lamps with the ambient gas temperature of 500 °C. In the 3rd and 4th zones of the post-heating section, the lamp intensity fractions further decreases to 0.0 for both the upper and lower lamps with the ambient gas temperature of 400 °C. Thus, the dielectric surface temperature keeps decreasing along the horizontal direction and the decreasing trend of the surface temperature in the post-heating section is generally similar to the increasing trend in the pre-heating section. The surface temperature at the 1st and 2nd zones of the post-heating section decreases rapidly and then approaches the uniform value closed to the ambient gas temperature. The surface temperature at the 3rd and 4th zones of the post-heating section decreases in the trend similar to the temperature variation at the 1st and 2nd zones of the post-heating section.

The main difference between the processes A and B for the panel of 0.632 m size is in the value of the lamp intensity fraction. The lamp intensity fractions of the process B in the pre-heating and post-heating sections are mostly larger than those of the process A. However, the differences of the lamp intensity fractions between the processes A and B in the post-heating section are not large when compared to those of the pre-heating sections as shown in Table 2. Thus the dielectric surface temperatures for the process B are mostly larger than those for the process A, especially at the 3rd and 4th zones of the pre-heating section and the RTP section. The general trend in the variation of the dielectric surface temperature for the process B is similar to that for the process A, which shows the rapid increase or decrease of the temperature followed by the almost uniform value.

In Fig. 8, the temperature distribution at the center on the dielectric surface as a function of time for two panels of 0.12 and 0.632 m sizes is shown to investigate the effects of the panel size on the temperature history during the process A. As shown in Tables 2 and 3, the lamp intensity fractions and ambient gas temperatures for the panel of 0.12 m size are the same as those for the panel of 0.632 m size. However, the process lengths and transport velocities for the panel of 0.632 m are larger

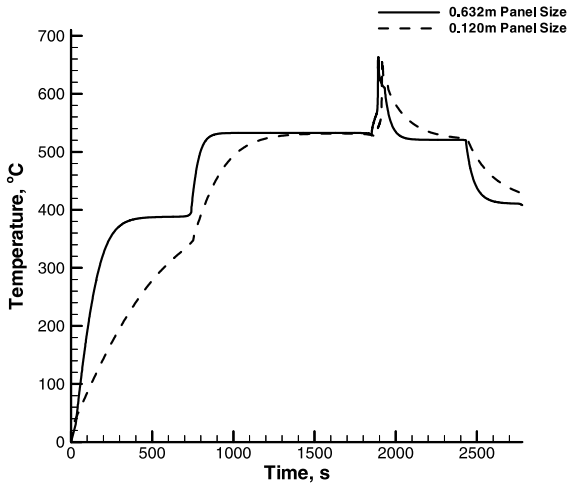

Fig. 8. Dielectric surface temperature variation as a function of time for different panel sizes of 0.120 m and 0.632 m for the type A process.

than those for the panel of 0.12 m size. At the 1st and 2nd zones of the pre-heating section, the dielectric surface temperature of the smaller panel (0.12 m size) increase rapidly. However, because the process length of 0.528 m at the 1st and 2nd zones is not long enough for the dielectric surface temperature to reach the ambient gas temperature of 400 °C, the uniform temperature period for the smaller panel is short, but the period for the larger panel (0.632 m size) is relatively long. At the 3rd and 4th zones of the pre-heating section, the surface temperature of the smaller panel increases rapidly again in the early part of the 3rd zone and then approaches the uniform value close to the ambient gas temperature due to the enough process length of 0.792 m. At the RTP section, the surface temperature variation for the smaller panel shows the pattern similar to that for the larger one. The surface temperature increases very rapidly in the early part, reaches the maximum, and then decreases gradually in the remaining part since the opaque dielectric is changed to the semi-transparent one. In the

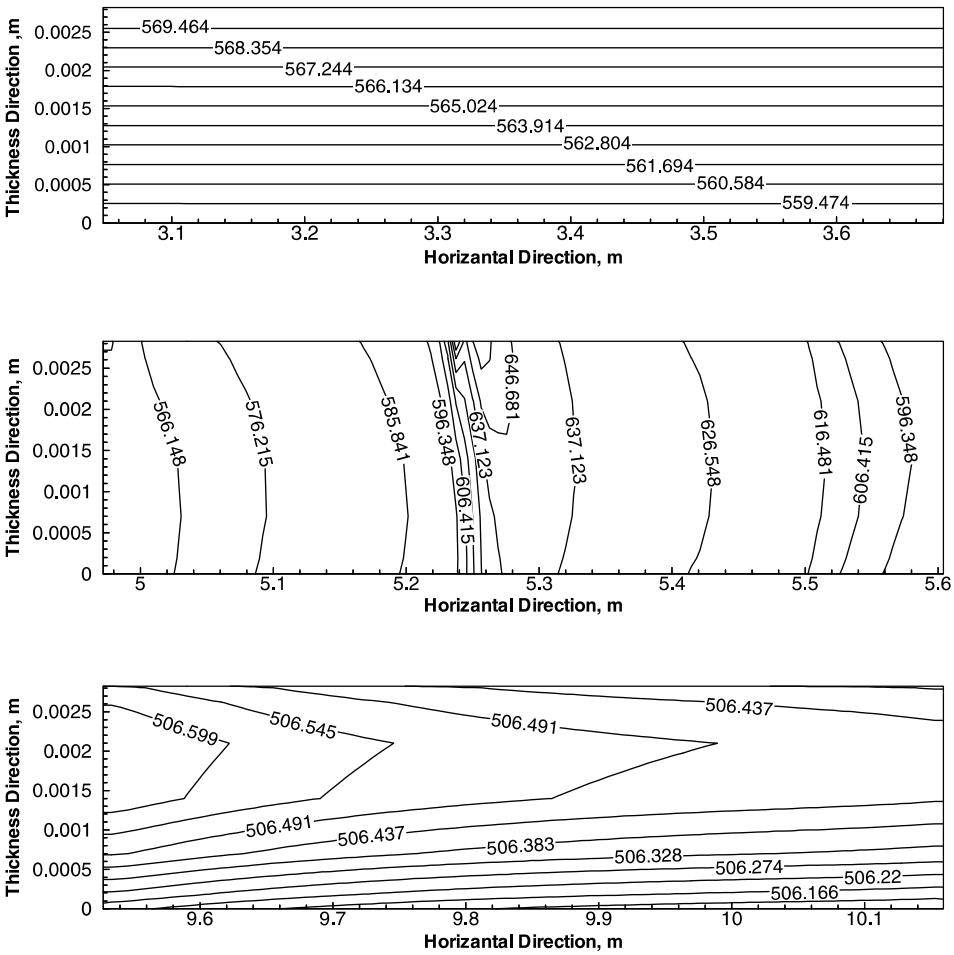

Fig. 9. Temperature distribution in the panel size for the 0.632 m panel size for the type A process.

post-heating section, the surface temperature for the smaller panel gradually decreases and the uniform temperature period is not shown due to the short process length. Using the operating conditions for the smaller panel given in Table 3, the process length may not be long enough for the panel to maintain the uniform temperature during a longer period that may be important in the viewpoint of the annealing process, thermal stress and displacement. The results show that the temperature distribution in the panel depends strongly on the operating conditions, which are functions of the panel size, transport velocity, lamp intensity, lamp arrangement, process length, etc. Thus, in order to decide the operating conditions for the RTP annealing process, it seems to be very useful to carry out the numerical simulations to choose the optimal condition.

Fig. 9 shows the isotherms in the panel of the 0.632 m size for the process A indicated in Table 2 in the pre-heating, RTP and post-heating sections while it moves in the horizontal direction. The temperature distribution of the panel in the pre-heating section is almost uniform as shown in Fig. 9(a). The temperature variation in the thickness direction is about 2–3 °C and the variation in the horizontal direction is almost uniform. As the panel approaches the RTP section as shown in Fig. 9(b), the temperature of the panel increases with increasing lamp intensities along the horizontal direction and reaches the maximum. After the RTP section, the temperature decreases with decreasing lamp intensities along the horizontal direction. Thus, the temperature variation in the horizontal direction is very large at the RTP section. In addition, the temperature differences in the thickness direction before and after the RTP section are not large but is very large in the RTP section, especially at the regions close to the dielectric surface. Since the dielectric is opaque to radiation in the RTP section when the temperature is less than 650 °C, the radiation incident on the dielectric surface from the upper xenon lamps is not

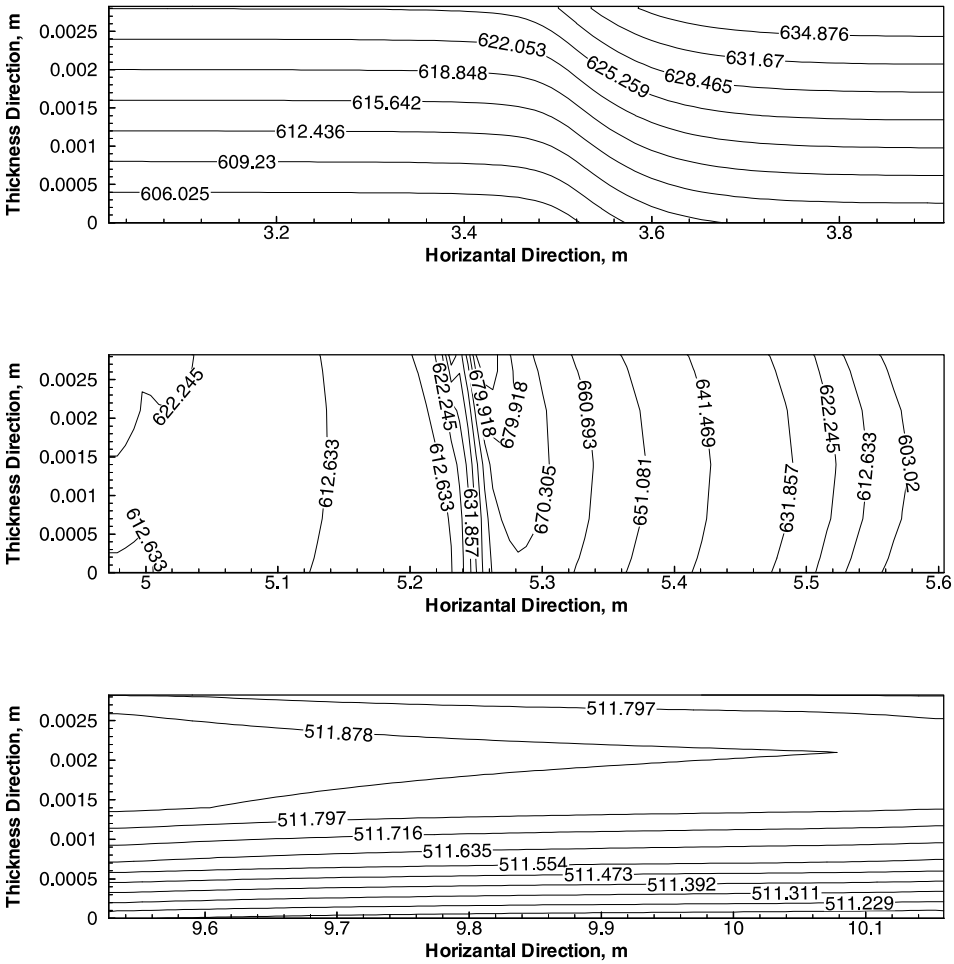

Fig. 10. Temperature distribution in the panel size for the 0.632 m panel size for the type B process.

transmitted through the dielectric medium but absorbed only at the surface. The radiation incident on the lower surface of the glass substrate from the lower xenon lamps is transmitted and absorbed through the semi-transparent glass. The radiation incident on the interface between the dielectric surface and the glass after being transmitted through the glass is absorbed and reflected at the interface, which causes the temperature at the location close to the interface to increase and to be the maximum. The maximum temperature difference through the thickness at this position is about 50 °C as shown in Fig. 9(b). Fig. 9(c) shows the temperature distribution in the panel at the post-heating section. The temperature in the panel is nearly uniform around 506 °C in both horizontal and thickness directions. As shown in Fig. 9, the large temperature gradient occurs in the RTP section due to the rapid heating in this region. Thus, the thermal stress and displacement in the RTP section are very larger than those in the pre-heating and post-heating sections, and may be larger than those to be required for the safe operation without any damages in the panel.

Fig. 10 shows the temperature distribution in the panel of the 0.632 m size for the process B. The positions of the panel in the pre-heating, RTP and post-heating sections for the process B are the same as those for the process A. The temperature distribution in the panel for the process B is generally similar to that for the process A. However, the temperatures for the process B are slightly larger than those for the process A because the lamp intensities for the process B is higher than those for the process A.

Fig. 11 shows the temperature distribution in the panel of 0.12 m size for the process A when the panel is placed in the pre-heating, RTP and post-heating sections. As shown in Fig. 8, the process lengths in the pre-heating and post-heating sections are not long enough to maintain the uniform temperature under the operating conditions for the panel of 0.12 m size given in Table 2. Thus, the temperature distribution of the panel in the

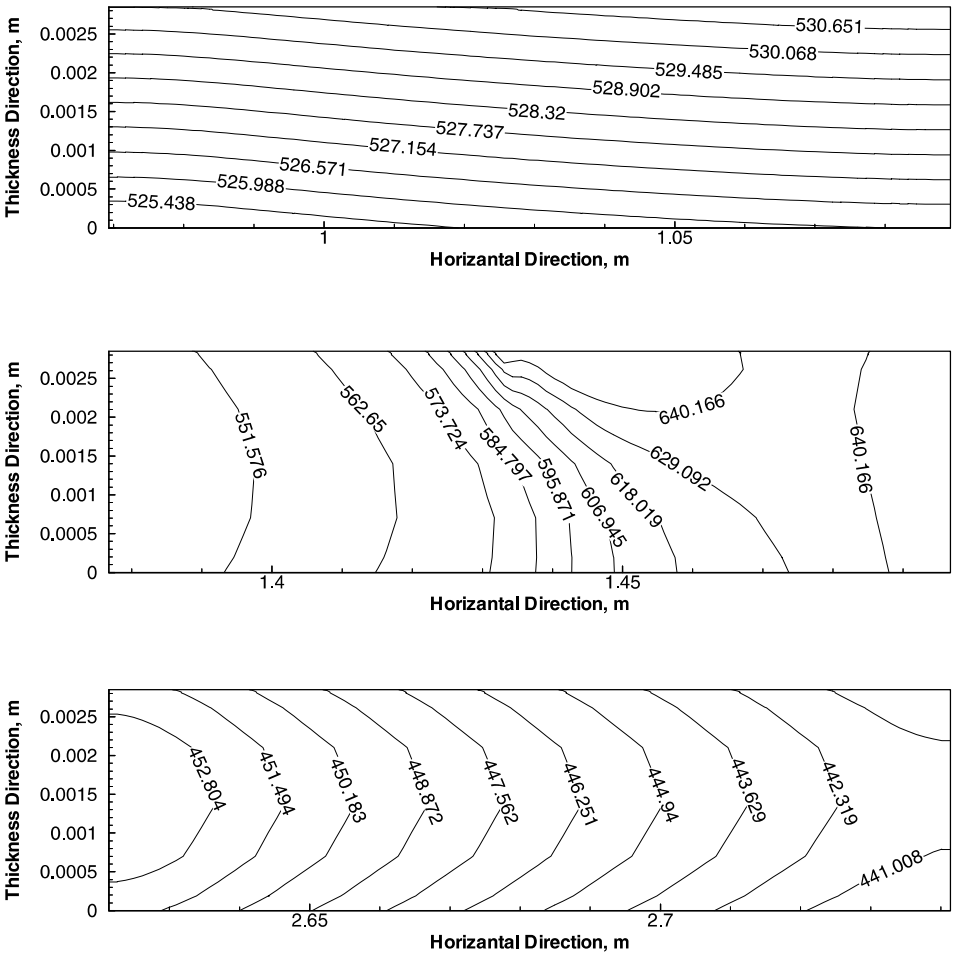

Fig. 11. Temperature distribution in the panel size for the 0.120 m panel size for the type A process.

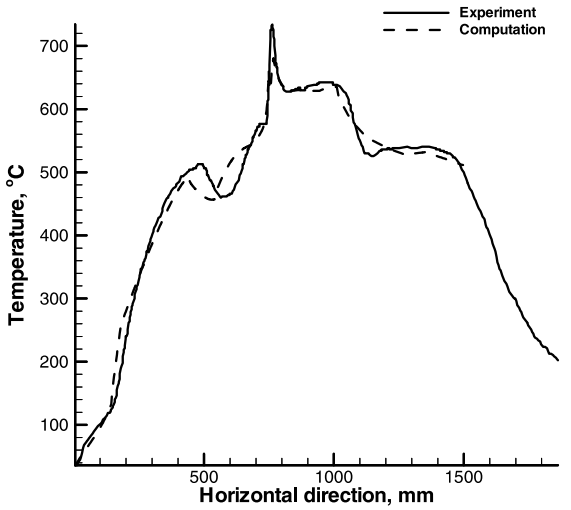

Fig. 12. Comparison of computational results for the dielectric surface temperature variation along the horizontal direction with experimental ones for the 0.12 m panel size.

pre-heating and post-heating sections is not uniform and shows slightly larger temperature difference than that for the panel of 0.632 m size in the horizontal and thickness directions. The temperature distribution of the panel in the RTP section is similar to that for the panel of 0.632 m size and the large temperature differences in the horizontal and thickness directions occur in the RTP section due to the rapid heating.

Fig. 12 shows the computational and experimental results for the temperature variation at the center of dielectric surface along the horizontal direction for the panel of 0.12 m size. The computational result agrees well with experimental one, showing the validity of the present computation.

4. Conclusions

A two-dimensional and unsteady computer program has been developed to analyze the combined conductive and radiative heat transfer in the annealing process using the RTP system. The finite volume and discrete ordinates methods are used to solve the energy conservation and radiative transfer equations, respectively. The radiative properties for the heating sources and panel are given by a function of wavelength.

In the pre-heating section, the panel temperature initially increases rapidly and then maintains the uniform value. The process is repeated depending on the operating conditions of lamp intensity, panel transport velocity, process length, ambient gas temperatures, etc. The general trend of decreasing panel temperature in the post-heating section is similar to that of increasing in the pre-heating section. The temperature in the RTP section increases very rapidly first due to the intensive radiant heating by the xenon lamps and reaches the maximum. However the temperature decreases after the opaque dielectric is changed to the semi-transparent medium.

The temperature differences/gradients of the panel in the horizontal and thickness directions are small in the pre-heating and post-heating sections but are very large in the RTP section, which may result in the large thermal stress and displacement to cause the considerable damage of the panel.

The temperature distribution in the panel depends strongly on the operating conditions. Thus, the simulations using the present computer program are useful to obtain the optimal operating conditions and to produce the panel of good quality.

Acknowledgements

This work was supported by LG Production Engineering Research Center. We wish to express our appreciation for the financial support provided by LG Production Engineering Research Center. This work was also partially supported by the Brain Korea 21 project. The computation presented here are performed with computer support from High Performance Supercomputing Cluster of RIBS and CREL of Pusan National University.

References

[1] R. Singh, Rapid isothermal processing, J. Appl. Phys. 63 (1988) 59–114.
[2] T.O. Sedgwick, Rapid thermal processing: how well is it doing and where is it going? Mater. Res. Soc. Symp. Proc. 92 (1987) 3–12.
[3] A. Lietoila, R.B. Gold, J.F. Gibbons, Temperature rise induced in Si by continuous arc lamp radiation, J. Appl. Phys. 53 (2) (1982) 1169–1172.
[4] C.M. Kyung, Temperature profile of a silicon-on-insulator multilayer structure in silicon recrystallization with incoherent light source, IEEE Trans. Electron Dev. ED 31 (12) (1984) 1845–1851.
[5] K.H. Lee, R. Viskanta, Prediction of spectral radiative transfer in a condensed cylindrical medium using discrete ordinates method, J. Quantitative Spectrosc. Radiat. Transfer 58 (1997) 329–345.
[6] M.F. Modest, Radiative Heat Transfer, McGraw-Hill, Highstown, NJ, 1993.
[7] B. Song, R. Viskanta, Deicing of solids using radiant heating, J. Thermophys. 4 (1990) 311–317.
[8] U. Gross, K. Spindler, E. Hahne, Shapefactor-equations for radiation heat transfer between plane rectangular surfaces of arbitrary position and size with parallel boundaries, Lett. Heat Mass Transfer 8 (1981) 219–227.
[9] D. Mann, R.E. Field, R. Viskanta, Determination of specific heat and true thermal conductivity of glass from

dynamic temperature data, Wärme- und Stoffübertragung 27 (1992) 225–231.
[10] V.I. Primencho, Theoretical method of determining the temperature dependence of the thermal conductivity of glasses, Glass Ceram. 37 (1980) 240–242.
[11] D.E. Sharp, L.B. Ginter, Effect of comparison and temperature on the specific heat of glass, J. Am. Ceram. Soc. 34 (1951) 260–271.
[12] M. Rubin, Optical properties of soda lime glasses, Solar Energy Mater. 12 (1985) 275–288.
[13] K.H. Lee, R. Viskanta, Two-dimensional combined conduction and radiation heat transfer: Comparison of the discrete ordinates method and the diffusion approximation methods, Numer. Heat Transfer, Part A 39 (2001) 205–225.
[14] S.V. Patankar, Numerical Heat Transfer and Fluid Flow, Hemisphere, Washington, DC, 1980.